High-Harmonic Generation of Attosecond Pulses in the "Single-Cycle" Regime

Ivan P. Christov,* Margaret M. Murnane, and Henry C. Kapteyn†

Center for Ultrafast Optical Science, University of Michigan, Ann Arbor, Michigan 48109-2099

(Received 30 September 1996)

High-harmonic generation with excitation pulses shorter than 25 fs is studied theoretically using a 3D model. For very short excitation pulses, a new regime of harmonic generation by a "single-cycle" of the driver pulse can be reached. In this regime, the temporal coherence of the adjacent harmonic orders is dramatically improved compared with longer excitation pulses, even though the discrete harmonic structure in the emission disappears. X-ray pulses as short as 100 attoseconds can be emitted, with increased conversion efficiency of laser-to-harmonic radiation. [S0031-9007(97)02387-9]

PACS numbers: 42.65.Re, 32.80.Rm, 42.50.Hz, 42.65.Ky

Extremely short-duration coherent soft x rays can be produced by focusing a high-intensity femtosecond laser pulse onto gases, clusters, and solids [1–6]. High harmonics of the exciting laser are produced in the forward direction, which can extend up to order 135. This process thus up-shifts a femtosecond pulse from the visible into the soft-x-ray region of the spectrum.

Most experiments to date have used $\approx$100 fs laser pulse widths to generate high harmonics. More recently, we used laser pulses as short as 26 fs to extend the wavelength range of the emitted harmonics, to increase the conversion efficiency of laser to x rays, and to increase the tunability of the soft-x-ray source [4,7]. However, low-energy pulses with pulse widths shorter than 26 fs have already been generated [8], and it is reasonable to assume that amplified sub-10 fs pulses at the intensities required for harmonic generation (typically 10^{15} W cm^{-2}) will be available in the near future. Thus, further improvements in coherent soft-x-ray generation will soon be possible.

A simple picture can be used to qualitatively understand high-harmonic emission [9,10]. The intense laser pulse ionizes the outer electron in an atom, by suppressing the Coulomb barrier binding the electron to the atom, so that the electron can tunnel through the core potential [11]. Once free, the electron moves in the field of the laser, to gain a maximum energy of $3.17U_p$, where $U_p = E^2/4\omega^2$ is the quiver energy of a free electron in the optical field of amplitude E and frequency ω. When the laser field reverses, the electron can reencounter the atom, and emit high harmonics if it undergoes stimulated recombination with the parent ion. Thus, the energy of the highest harmonic emitted by the atom is predicted semiclassically to be $I_p + 3.17U_p$, where I_p is the ionization potential of the atom. This cutoff rule has been confirmed experimentally for pump pulses longer than 100 fs, but for shorter pulses (i.e., sub-25 fs) it does not apply, since then the amplitude of the excitation pulse changes significantly during the generation of each individual harmonic, and hence the value of E which determines U_p is not precisely known [4]. Moreover, in recent work, we demonstrated that when the pump pulse duration approaches the period of the optical pulse, and the Keldysh parameter is close to unity, the atom exhibits a nonadiabatically delayed response, which reduces the ionization "rate" [7].

In this Letter, we theoretically model harmonic generation by intense pulses with durations of 5–25 fs. We find that a completely new regime of interaction is reached for the shortest excitation pulses, when a *single cycle* of the excitation pulse drives harmonic emission over a range of adjacent harmonic orders. As a result, the temporal coherence of the harmonics is dramatically improved compared with longer excitation pulses, and more efficient x-ray pulses, with durations as short as 100 attoseconds, can be emitted. This behavior is unique to very short excitation pulses, because even for the case of a 25 fs laser pulse (10 cycles FWHM), the high harmonics are generated during more than two periods of the optical pulse. That means that in the simple semiclassical picture, the electron reencounters the core more than two times, which leads to the observation of relatively broad but still discrete harmonics. However, the subsequent reencounters perturb the phase relation between the different portions of the harmonic spectrum, which are generated at different times during the process of ionization. This results in a decrease in coherence of the harmonics for pulses of duration 25 fs or longer.

Our analysis is based on a numerical solution of the Schrödinger equation (in atomic units), for an electron in a smoothed 3D Coulomb potential:

$$i\,\frac{\partial}{\partial t}\,\psi(\mathbf{r},t) = \left[-\frac{1}{2}\,\Delta - \frac{1}{r+\alpha} + \mathbf{r}\cdot\mathbf{E}(t)\right]\psi(\mathbf{r},t)\,. \tag{1}$$

In contrast to previous work [12,13], in Eq. (1) we use a smoothing parameter α, in order to make the calculation insensitive to the size of the spatial step. For linearly polarized light along the z axis, we expand the wave function in spherical harmonics:

$$\psi(\mathbf{r},t) = \sum_{l=0}^{\infty} \frac{1}{r}\,R_l(r,t)Y_l^0(\theta)\,. \tag{2}$$

This reduces Eq. (1) to a set of coupled equations for the radial wave function $R_l(r,t)$ [12,13]:

$$i\frac{\partial}{\partial t}R_l(r,t) = \left[-\frac{1}{2}\frac{\partial^2}{\partial r^2} - \frac{1}{r+\alpha} + \frac{l(l+1)}{2(r+\alpha)^2}\right] \times R_l(r,t) + rE(t) \times [c_l^+ R_{l+1}(r,t) + c_l^- R_{l-1}(r,t)], \quad (3)$$

where c_l^+ and c_l^- are parameters related to the Clebsch-Gordon coefficients.

In the 1D case, where $l = 0$ and $-\infty < r < +\infty$, and for no external field, Eq. (3) possesses a doubly-degenerate set of normalized bound-state eigenfunctions with even and odd parity. For small values of the smoothing parameter α, the eigenfunctions are close to those of hydrogen [14]. We use $\alpha = 0.037$ a.u., for which the even bound states have energies (in a.u.) of -18.9, -0.359, -0.105, -0.0492, etc., while the odd bound states have energies -0.443, -0.117, -0.0532, etc. The most deeply bound even state (-18.9 a.u.) is unphysical [14], and is not connected to other states through dipole transitions. In the 3D case, where $0 \leq r < \infty$, there are no even bound states, and all radial eigenfunctions $R_{nl}(r)$ are zero at the core. We calculate the radial eigenfunctions for a given value of α. The ionization probability is then calculated from

$$P(t) = 1 - \sum_{nl}\left|\int R_{nl}(r)R_l(r,t)r\,dr\right|^2, \quad (4)$$

while the scattered field is estimated by using the expectation value of the dipole acceleration:

$$E_r(t) \propto \sum_l \int_0^\infty \frac{c_l^+ R_l^*(r)R_{l+1}(r) + c_l^- R_l^*(r)R_{l-1}(r)}{(r+\alpha)^2}\,dr\,. \quad (5)$$

Equation (3) is solved by an efficient split-step technique, where the diffusion operator is taken by a fast Fourier transform, and the time evolution due to the coupling between the different channels $l-1, l, l+1$, is calculated by a fourth-order Runge-Kutta scheme. Here we use up to 25 channels for the angular momentum l.

Figure 1(a) shows the harmonic spectrum of a 25 fs laser pulse, with a peak intensity of 1.1×10^{15} W/cm^2 ($E = 0.18$ a.u.). It can be seen that the harmonic peaks are still distinguishable for such a short pulse, although there is observable broadening of the peaks and noise between the peaks. (For 100 fs laser pulses of the same peak intensity, the harmonic peaks are half the width on a log scale.) In order to test the validity of the $I_p + 3.17U_p$ rule, in Fig. 1(b) we plot the time dependence of the 51st harmonic (obtained by a Fourier transform of the corresponding spectral amplitude). We see that the harmonic is generated during $\approx$3 cycles of the laser pulse, during which time the ionization probability varies from 10% to $\approx$100%. During this time also, the amplitude of the incoming pulse changes by $\approx$30%, and therefore

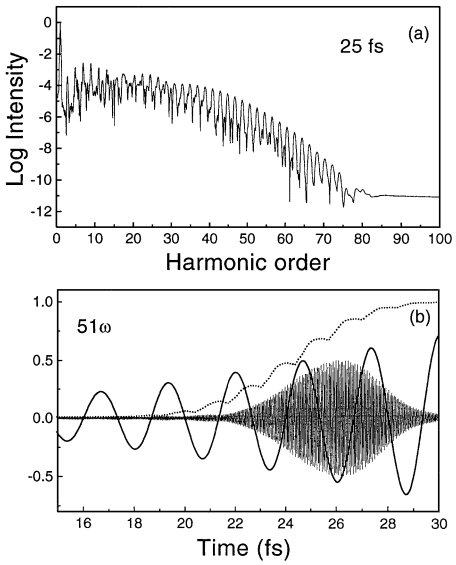

FIG. 1. (a) Harmonic spectrum of a 25 fs laser pulse with peak intensity 1.1×10^{15} W/cm^2. (b) Time dependence of the normalized laser field (bold line), ionization probability (dashed line), and the normalized 51st harmonic (thin line).

the E field to use is ambiguous. We choose a value of the field of $\approx$0.108 a.u., which corresponds to the field at the peak of the harmonic. The $I_p + 3.17U_p$ rule yields a value of 57 for the number of harmonics in this case. However, from Fig. 1(a) it is clear that for a 25 fs laser pulse, there is no sharp cutoff of the harmonic spectrum, as is the case for longer pulses. Therefore, the $I_p + 3.17U_p$ gives a rough estimate for the width of the harmonic plateau only when we know in advance the value of the instantaneous intensity at which the harmonics are generated.

In order to study high harmonic generation occurring over a time period of less than 2 optical cycles, we calculated the harmonic output for a 10 fs excitation pulse with an intensity of 1.1×10^{15} W/cm^2, shown in Figs. 2(a)–2(c). The discrete nature of the harmonics is smeared, especially for the higher orders, an effect which can be attributed to the broad bandwidth of the driving pulse which is mixed by the nonlinear atomic response. In addition, there are several spectral regions, separated by sharp drops in the harmonic intensity, positioned at 30th, 50th, and 70th harmonics. Figures 2(b) and 2(c) show the time dependence of the emission from these regions, and show that the spectral components of these bands are generated during different cycles of the laser pulse. Therefore high-harmonic generation by a very short pulse ensures good correspondence between the time and frequency history of the harmonic spectrum. This effect can be used to control the properties of the high harmonics. These effects become even more pronounced for harmonic generation by a 5 fs laser pulse, as shown in Figs. 2(d), 2(e), and 2(f). In this case we observe a fewer number of bands in the

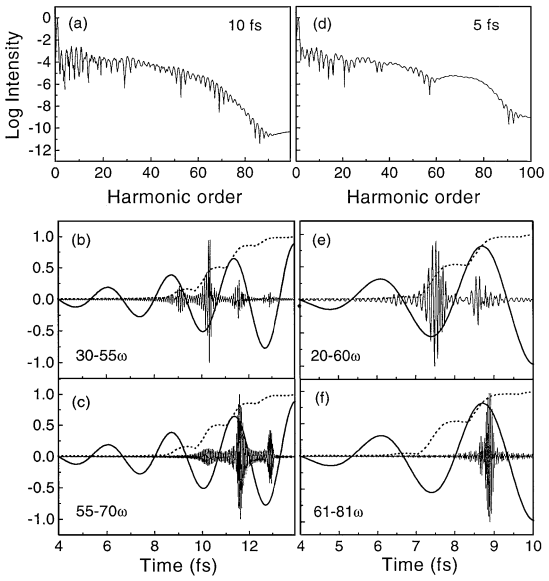

FIG. 2. (a) Harmonic spectrum of a 10 fs laser pulse with peak intensity 1.1×10^{15} W/cm^2. (b) Time dependence of the laser field (bold line), ionization probability (dashed line), and the superposition of harmonics 30–55. (c) As in (b) for harmonics 55–70. (d) Harmonic spectrum of a 5 fs laser pulse with peak intensity 1.1×10^{15} W/cm^2. (e) Time dependence of the laser field (bold line), ionization probability (dashed line), and the superposition of the harmonics 20–60. (f) As in (b) for the harmonics 61–81. Note that the fundamental and harmonic fields are normalized in arbitrary units because of the very large difference between the corresponding absolute values.

spectral domain [Fig. 2(d)], and the harmonic structure almost disappears. This implies that the harmonic generation occurs during very few reencounters of the electron with the core [15]. Figures 2(e) and 2(f) show the time dependence of the radiation corresponding to the spectral band between the 20th and 60th harmonics, and between the 61st and 81st harmonics, respectively. A comparison between Figs. 2(b) and 2(c) and Figs. 2(e) and 2(f) shows that for a 5 fs pulse, there is almost a unique correspondence between the frequency and time evolution of the harmonic emission. Moreover, Fig. 2(f) shows that the spectrum between the 61st and 81st harmonics corresponds to a sub-500 attosecond pulse in the time domain. Moreover, the attosecond duration is quite insensitive to the exact spectral bandwidth selected, and therefore should be relatively easy to implement experimentally with good efficiency by separating the appropriate spectral band using either filters or broadband x-ray mirrors. Other schemes proposed for attosecond pulse generation require the use of elliptically polarized light [16] or other compression techniques [17]. Figures 2(e) and 2(f) also show that the atomic ionization which occurs does not strongly perturb the phase relationships between the harmonics. Although there is significant ionization prior to the attosecond pulse generation [Fig. 2(f)], for these sufficiently short laser pulses the harmonic field generated during each reencounter only weakly depends on the history of the interaction (i.e., previous reencounters). Therefore there is no need to require a single-reencounter regime in order to generate attosecond pulses [15].

Another advantage of using shorter pulses is that the ionization saturates at relatively high values of the field [see Figs. 1(b), 2(b), and 2(e)] and hence the harmonic spectrum extends to much higher frequencies. We observe that for shorter pulses, a redistribution of the energy between the different harmonic orders occurs, where the lower orders are weaker, while the higher orders are stronger, than for longer pulses. The suppressed ionization for shorter pulses is due in part to the nonadiabatic response of the atom to the rapidly increasing electric field [7]. First we note that in 3D, the nonadiabatic response of the atom manifests itself for shorter pulse durations than for 1D, since in 3D, a large portion of the electron cloud misses the nucleus, and does not experience as strong an acceleration as for the 1D case. To illustrate these 3D effects for different pulse durations, Fig. 3 shows the correspondence in time between the incoming pulse and the dipole moment of the atom at the fundamental frequency, for the case of a 100 fs pulse and a 10 fs pulse. It is clear that for the 100 fs pulse, the two waves are in phase for values of the ionization up to 100%, while for the 10 fs pulse, there is a phase lag of the dipole moment with respect to the incident laser field at values well below full ionization of the atom. Physically what is happening is that during tunneling, a portion of the electron cloud remains trapped in intermediate states, as shown in Fig. 4. Although in order to calculate the population of the first excited state in Fig. 4, we use a projection on the bare atomic state, we assume that during the subsequent periods of the laser field the trapped portion of the electron cloud takes part in the subsequent harmonic generation via

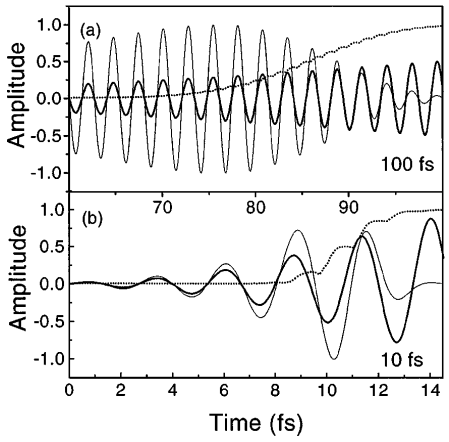

FIG. 3. Time dependence of the normalized laser field (bold line), the dipole moment at the fundamental frequency (thin line), and the ionization probability (dashed line) for (a) a 100 fs laser pulse and (b) a 10 fs laser pulse.

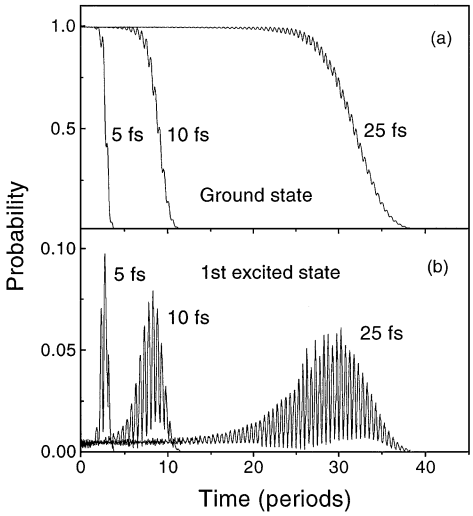

FIG. 4. Time dependence of the population of (a) the ground state, and (b) first excited state of the atom for different pulse durations.

a series of cascade Raman transitions between the dressed atomic states. This effect contributes to the higher efficiency of harmonic conversion for shorter pulses.

In order to investigate changes in the harmonic generation process across the laser beam, as the intensity decreases due to the Gaussian shape, we checked the model predictions for intensities of 10^{14} and 5×10^{14} W/cm^2. We found good temporal synchronization between the peaks of the radiated field in both cases, i.e., a strong attosecond peak appears at the same moment in time as in Fig. 2(f). However, for lower intensities the main peak is surrounded by weaker peaks, corresponding to emission from adjacent periods of the laser pulse. Therefore, a flat-top spatial distribution would be used to generate the attosecond x-ray pulses in the actual experiment.

In conclusion, using a 3D model we demonstrated that it is possible to generate an attosecond soft-x-ray pulse, using the process of high-harmonic generation with sub-10 fs laser pulses. Using such short driving pulses, the harmonic emission becomes very broad spectrally, and the highest orders almost merge together. However, the temporal coherence of these higher merged harmonics is higher than that of the lower-order discrete harmonics. Thus, these harmonics can be spectrally selected using a simple broadband x-ray filter to produce ≈100 attosecond duration x-ray pulse widths.

The authors thank Andrew Rundquist for invaluable help. The authors acknowledge support for this work from the National Science Foundation. H. K. acknowledges support from an Alfred P. Sloan Foundation Fellowship.

*Permanent address: Department of Physics, Sofia University, 1126 Sofia, Bulgaria.
†Electronic address: kapteyn@eecs.umich.edu

[1] A. McPherson, G. Gibson, H. Jara, U. Johann, T. S. Luk, I. A. McIntyre, K. Boyer, and C. K. Rhodes, J. Opt. Soc. Am. B **4**, 595 (1987).
[2] J. J. Macklin, J. D. Kmetec, and C. L. Gordon III, Phys. Rev. Lett. **70**, 766 (1993).
[3] A. L'Huillier and P. Balcou, Phys. Rev. Lett. **70**, 774 (1993).
[4] J. Zhou, J. Peatross, M. M. Murnane, H. C. Kapteyn, and I. P. Christov, Phys. Rev. Lett. **76**, 752 (1996).
[5] T. Ditmire, T. Donnelly, R. W. Falcone, and M. D. Perry, Phys. Rev. Lett. **75**, 3122 (1995).
[6] P. Gibbon, Phys. Rev. Lett. **76**, 50 (1996).
[7] I. P. Christov, J. P. Zhou, J. Peatross, A. Rundquist, M. M. Murnane, and H. C. Kapteyn, Phys. Rev. Lett. **77**, 1743 (1996).
[8] J. Zhou, G. Taft, C. P. Huang, M. M. Murnane, H. C. Kapteyn, and I. Christov, Opt. Lett. **19**, 1149 (1994).
[9] P. B. Corkum, Phys. Rev. Lett. **71**, 1994 (1993).
[10] K. C. Kulander, K. J. Schafer, and J. L. Krause, in *Super Intense Laser-Atom Physics*, NATO ASI Ser. B, Vol. 316, edited by B. Piraux *et al.*, (Plenum, New York, 1993).
[11] L. V. Keldysh, Zh. Eksp. Teor. Fiz. **47**, 1945 (1964).
[12] K. J. LaGuttuta, J. Opt. Soc. Am. B **7**, 639 (1990).
[13] S. C. Rae, X. Chen, and K. Burnett, Phys. Rev. A **50**, 1946 (1994).
[14] U. Schwengelbeck and F. H. Faisal, Phys. Rev. A **50**, 632 (1994).
[15] M. Protopapas, D. G. Lappas, C. H. Keitel, and P. L. Knight, Phys. Rev. A **53**, 2933 (1996).
[16] M. Ivanov, P. B. Corkum, T. Zuo, and A. Bandrauk, Phys. Rev. Lett. **74**, 2933 (1995).
[17] K. Kulander (private communication).